PHOTOCATALYTIC DYE DEGRADATION EFFICIENCY OF HYDROTHERMALLY SYNTHESIZED NICKEL OXIDE NANOPARTICLES

Project report submitted to the

University of Kerala

In partial fulfillment of the requirements for the award of the degree of

MASTER OF SCIENCE IN PHYSICS

2020 - 2022

ABSTRACT

In this present study, Nickel oxide (NiO) nanoparticles have been synthesized by hydrothermal method and characterized using X-Ray Diffraction, UV-Vis Spectroscopy, and Scanning Electron Microscopy. The result of characterization indicated that synthesized sample has a pure cubic phase of NiO with an oval shape morphology. Test of photocatalytic activity of synthesized sample towards the model contaminant dye Rhodamine B (Rh B) shows a degradation efficiency of 89% in a period of 1 hour under natural sunlight. This value showed that the synthesized NiO possess better photodegradation efficiency of Rh B dye and it showed that particles synthesized at higher temperature hold good degradation efficiency than that with low temperature.

CONTENTS

CHAPTER 1
INTRODUCTION

1.1 Nanoscience

Nanoscience is an upcoming area of science which is the study, manipulation and engineering of matter and particles in nanometer scale. The origin of the word “Nano” is from the Greek word having the meaning “dwarf”. Nanoparticles are the structures with a dimension in a range of 1-100 nanometers, but in scientific jargon, it means one billionth [1]. Molecules and atoms assemble on nanoscale into larger structures. By this way, we can determine the important properties of material such as electrical, optical, thermal and mechanical properties.

Nanoscience is cross disciplinary and scientist in different fields like chemistry, physics, biology, medicine, material science, engineering are studying and using it. Nanoscience is having applications in our everyday life ranging from goods to medicines. The Nano dimensions have some features like large of surface area to volume ratio, large fraction of surface atoms to bulk. The small size makes many barriers transparent.

1.2 Nanotechnology

Nanotechnology (nanotech in short) is the utilization of matter on atomic, molecular and super molecular scale of industrial purpose. It is the field of applied science and technology whose centralizing theme is that the size of matter is controlled in range less than 1 micrometer, normally in the range of 1-100 nm, and therefore fabricating device within that size. Nanotechnology is a prominent engineering discipline that utilizes the knowledge in nanoscience to create functional, marketable and economically feasible products [1].

The term ‘nanotechnology’ was first explained in 1974 by Norio Taniguchi of Tokyo science University as “nanotechnology is the process of separation, consolidation and deformation of materials by one atom or one molecule”.

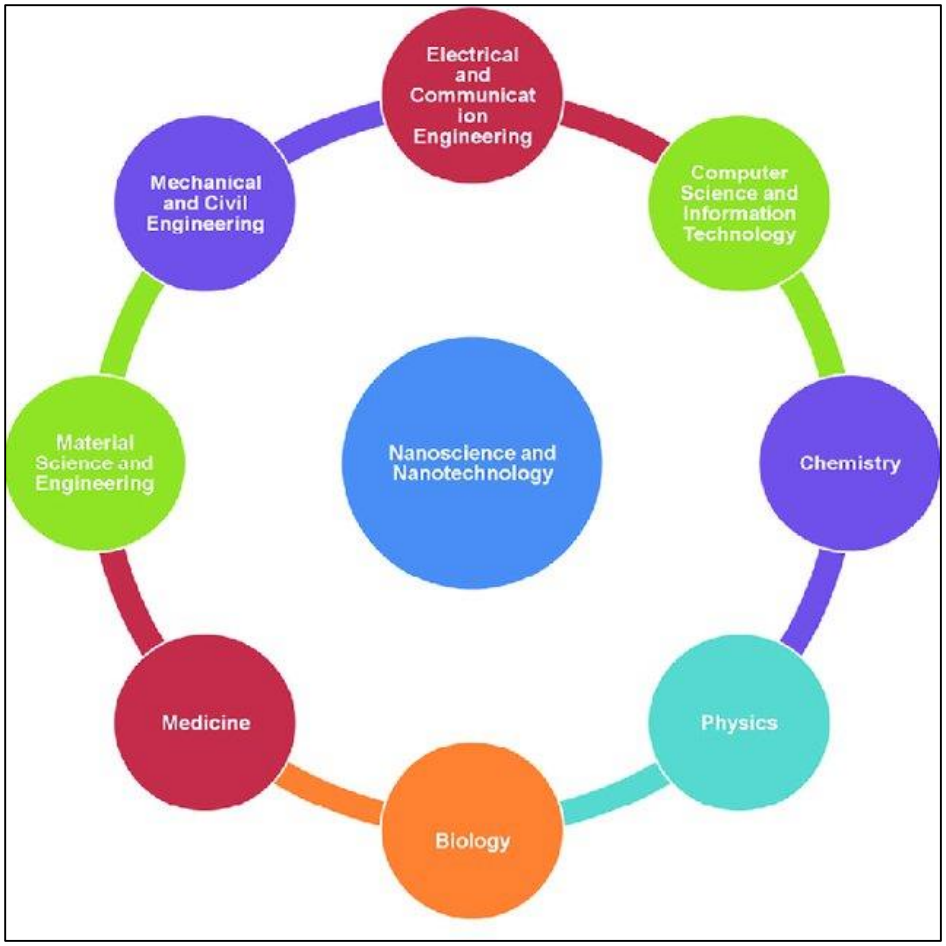

Figure.1.1.Role of Nanoscience and Nanotechnology [2]

1.3 Concepts in Nanoscience and Nanotechnology

Nanoscience and nanotechnology is the capability to see and control individual atoms and molecules. Each and every thing around this Earth is made up of atoms. Everything we eat, we wear and where we live and even our own body are made up of tiny atoms. But it is not possible to see something that is very small as an atom with our naked eye. We now use microscopes to see things at the nanoscale which were actually invented in the early 1980s. Once scientists chose their right tools, like the Scanning Tunneling Microscope (STM) and the Atomic Force Microscope (AFM), the era of nanotechnology was born. Even if nanoscience and nanotechnology are quite new, the nanoscale materials were invented and used for centuries. About hundred years ago, people created colours in stained glass windows in medieval church using alternate sized gold and

silver particle. The artists who created these things were not aware that their creation actually led to change in composition of different materials they used [3].

Nowadays, many scientists and engineers find different ways to make materials at the nanoscale and use the advantage of their enhanced properties like high strength, light weight, and increased control of light spectrum, and their chemical reactivity.

1.4 History behind Nanotechnology

Artisans in 9th century in Mesopotamia were the first to create a glittering effect on surface of pots and thereby taken a first step towards nanotechnology. The shiny effects that they produced were due to presence of silver and copper nanoparticles. Another plot of history lays in hands of Romans for their discovery of Lycurgus cup (Figure 1.2) at AD 400. These cups were made of a glass that could change its color when we pass light through it. The glass was composed of Au-Ag alloyed nanoparticles, distributed in a way to make the glass looks green when light is reflected and red when light pass through it [3].

The first scientific report made by Michael Faraday in 1857 at Royal Society of London reported the synthesis of colloidal solution of gold nanoparticles called “activated gold”. According to him “gold reduced in exceeding fine particles, which becoming diffused, produce a ruby red fluid, the various preparation of gold, whether ruby, green, violet or blue consist of that substance in a metallic divided state” [4].

Later in 1959, there was a legendary talk on “there’s plenty of room at bottom: an invitation to enter a new field of physics” by Nobel Laureate Dr. Richard P. Feynman. He discussed the ideas of manipulation and control of things at atomic scale. He also commented these famous words “the principles of physics, as far as I can see, do not speak against the possibility of manoeuvring things atom by atom” [5]. Norio Taniguchi, in 1974, was the first one to use the term “nanotechnology” in his paper entitled “On the basic concept of nanotechnology” [6]. According to him “Nanotechnology mainly consist of processing, separation, consolidation, and deformation of materials by one atom or one molecule” [7].

Figure.1.2.The Lycurgus cup, an example of nanotechnology(British Museum, London)

1.5 Nanoparticles

Nanoparticles are the elementary components of nanotechnology. Its size ranges between 1 and 100 nanometres. These particles exhibit unique chemical, physical and biological properties compared to the bulk. This is due to relatively large surface area to volume, increased stability or reactivity in a chemical process and also due to their high mechanical strength. They may be made up of carbon, metal oxides or organic matter. Due to their distinguished properties the have a wide range of applications. Nanoparticles are not simple molecules and thus have three layers. (a) The surface layer which may be functionalized with a variety of small molecules, metal ions, surfactants and polymers (b) The shell layer which is chemically different material from the core in all aspects, and (c) The core, which is essentially the central portion of the nanoparticles and usually get refered as nanoparticle. Having these exceptional properties, nanomaterials got immense interest of researchers in multi-disciplinary fields [8].

Nanoparticles can have different shapes, sizes and structures. They can be spherical, cylindrical, tubular, conical, hollow, flat, spiral, etc. There can be surface variations also, like it may be regular or irregular. Some may be crystalline in nature while others may be amorphous with single or multi crystal solids either loose or agglomerated. Scientist came forward with different synthesis method to improve the properties of nanoparticle and at the same time to reduce the cost of production. Some methods are modified to achieve process-specific nanoparticles to increase therir optical, mechanical, physical and chemical properties. The development in fields of instrumentation also improved nanoparticle characterisation and subsequent application [9].

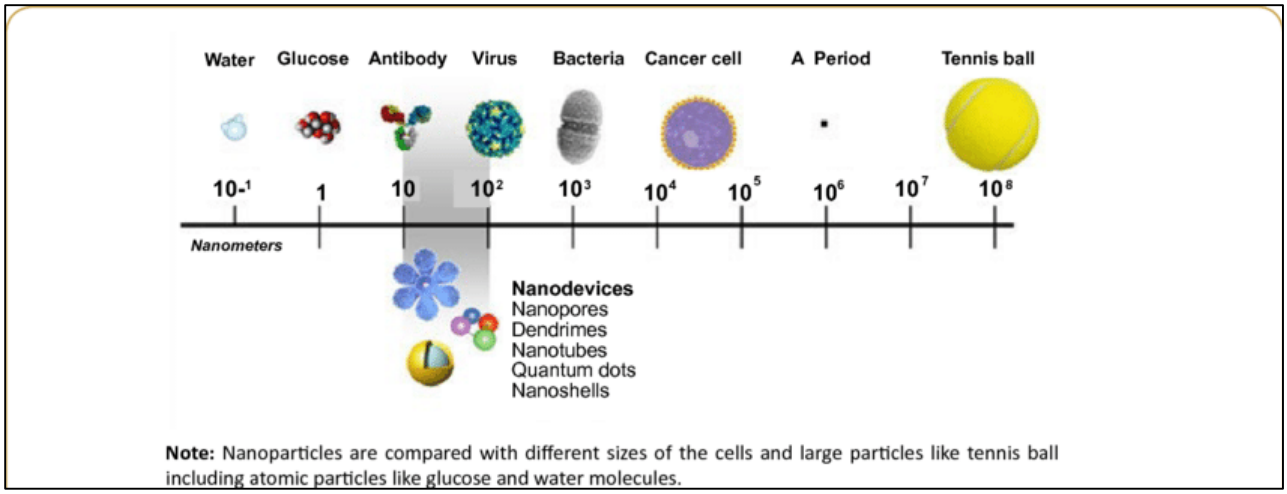

Figure.1.3 Size Comparison of nanoparticle [12]

1.6 Classification of nanomaterials

Nanomaterials are broadly classified into various groups based on the geometry, size, morphology and chemical properties of nanoparticles.

1.6.1 Based on dimensionality

- **Zero-dimensional (0-D) nanoparticles:** They all have dimensions less than 100 nm i.e.,the electron movement is confined in all directions. Such nanoparticles are called quantum dots. They include nanospheres and nano clusters.They can be single crystalline or polycrystalline. It can exist individually or incorporated in a matrix. Some of the examples are fullerenes, graphene quantum dots, carbon quantum dots etc.
- **One-dimensional (1-D) nanoparticles:** In these types of nanomaterials, one of the dimension will be outside the nanometer range i.e., they have two dimensions in the nanometre scale. The electron movement is thus confined in two directions. These types of nanoparticles are called quantum wells. These includes nanorods, nanowires, nanotubes and nanofibres. They are used in the circuitary of computer chips and hard coatings on the eyeglasses.
- **Two- dimensional (2-D) nanoparticles:** Here, two dimensions are outside the nanometre range. Thus the electron movement is confined in one direction. Such nanoparticles are called quantum wires. They include nanosheets, nanofilms, and nanoribbons. They are used

in electronics /optoelectronics, in sensors and in biomedicine because of their high mechanical stability and optical transparency.

- **Three – dimensional (3-D) nanoparticles:**They are outside the nanometre range.They are not confined to the nanoscale in all dimensions. Thus the electron can move in all directions i.e., electrons are completely delocalized. They are also called bulk nanomaterials composed of individual blocks which are in nanometre scale (1-100 nm).They have large surface area and posses a nanocrystalline structure.

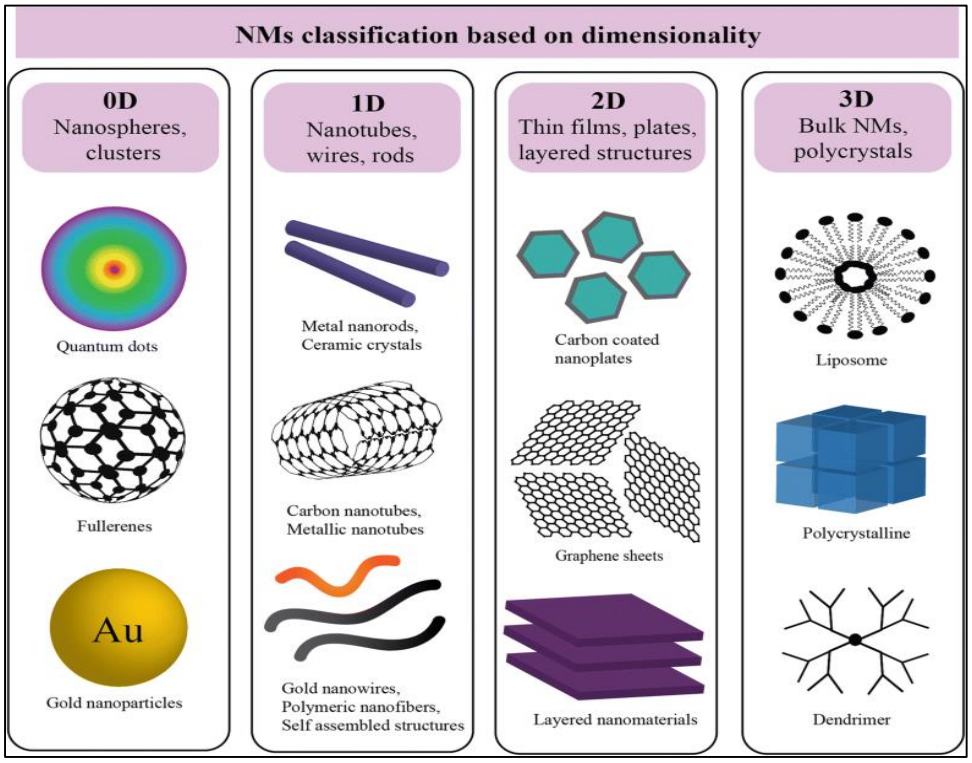

Figure.1.4 Classification of NM based on dimensions [10]

1.6.2 Based on morphology

Nanomaterials are classified into materials with high or low aspect ratio materials based on their morphology.

Their main characters include aspect ratio, flatness and sphericity [3].

- **High aspect ratio nanoparticles**: Nanotubes with shapes such as helices, zigzags, and belts.

- **Low aspect ratio nanoparticles**: Nanoparticles with different shapes such as helical, spherical, cubic, pillar and oval.

Most of these nanoparticles occur in the form of powder, suspensions or colloid**.**

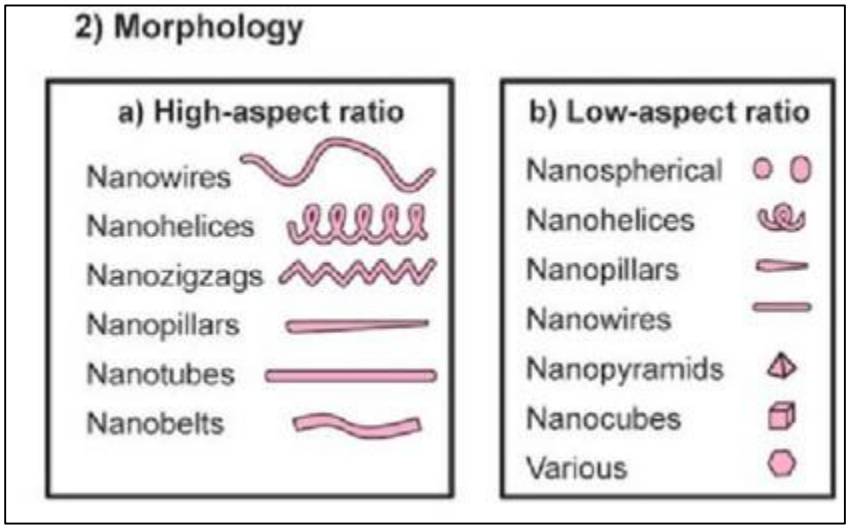

Figure.1.5 Classification based on morphology [11]

1.6.3 Based on composition

- **Carbon- based nanomaterials**: These nanomaterials composed of carbon and may have shapes like hollow spheres, tubes or ellipsoids. Cylindrical ones are called nanotubes and spherical or ellipsoidals are called fullerenes.

  Carbon nanofibres, carbon black, graphene is include in the category of carbon based nanomaterials.

  Fullerenes (C_{60}) are referred to "Buckyballs" which are made of carbon atoms with sp^2 bonds. Fullerenes are highly symmetric. They also shows non-linear optical responses due to the presence of delocalizded pi electrons.

  Carbon Nano Tubes (CNTs) can be single-walled, double walled or multi walled. They are arranged in zig-zag, armchair and chiral manner. It have properties like rigidity, strength, elasticity, conductivity, etc.

  Graphenes is another allotrope of carbon. It is a 2-D material having sp^2 hybridized carbon atoms. It is also called " miracale material" because of its super properties.

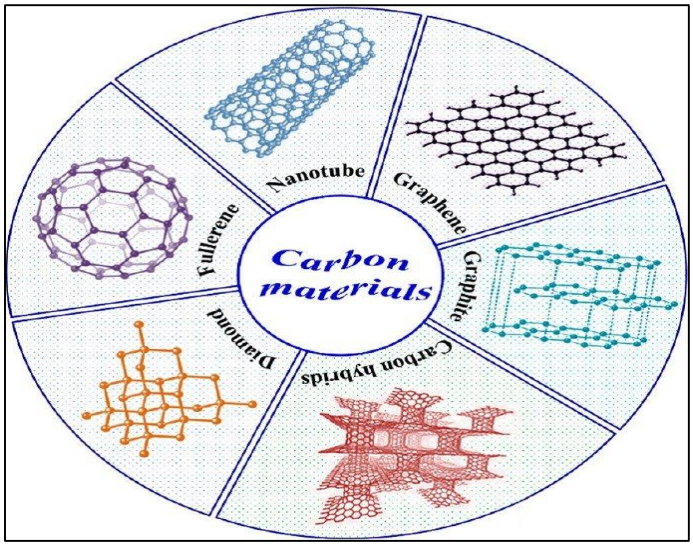

Figure.1.6 Carbon Baesd Nanomaterials

- **Organic based nanomaterials**: These nanomaterials are made of oragnic matters. They can be transformed into desired structures such as dendrimers, micelles, liposomes by using non-covalent interactions. These nanomaterials are biodegradable, non-toxic and are also sensitive to thermal and EM radiations. They have their applications in biomedical industries.
- **Inorganic based nanomaterials**: They include metals, metal oxides, and ceramic based nanomaterials. They also show many optical as well as electronic properties. Clays are natural inorganic nanomaterial which is formed by crystal growth in diverse chemical condition on Earth's crust. Inorganic quantum dots possess unique properties such a brightness, photostability, multicolour capability, etc.
- **Composite based nanomaterials**: Composites are made of two or more different materials that are blended to get best properties of each. They have multiple phases. In nature, nanocomposites are found in bones, eggshells, and abalone shells. They aim to create new materials with great flexibility and improved mechanical, physical, chemical and biological properties [11].

1.7 Propeties of nanomaterials

The properties of a material made of nanoparticle are unusually different from those of the bulk one even if it is divided into micrometer sized particles. Many of them may be due to spatial

confinement of sub-atomic particles like electrons, protons, etc. and electric fields around these particles.

1.7.1 Physical properties

This includes the optical properties like nanoparticle's colour, light penetration, absorption etc.,mechanical properties like elasticity, ductility, flexibility and other properties like hydrophilicity, hydrophobicity, suspension, diffusion, etc. The magnetic and electrical properties such as conductivity, semi-conductivity and resistivity have led to their use in modern electronics and renewable energy applications[8].

- **Optical properties**

  The optical activity in a nanomaterial can be obtained through different mechanisms, depending on the size, composition and arrangement of nanomaterial. These properties are independent to some extent. Noble metal nanoparticles have size dependent optical properties and a strong UV visible extinction band spectrum which is not seen in the bulk materials. When a metal absorbs light of resonant wavelength it will cause electron cloud to vibrate. This process normally happens at the surface of the particle and therefore they are called surface plasmon resonance. Oscillations of electron clouds are the plasmons. The incident photon frequency of the excitation band is constant with respect to the collective excitation of the conduction electron. Then it is called localized surface plasmon resonance. When the size of nano sphere is less than the wavelength of incident radiation then a resonance occurs and it will generate the surface plasmon resonance. During this time, the frequency of surface plasmon is equal to the frequency of radiation due to constructive interference. Localized surface plasmon resonance spectrum depends upon the size, shape, interatomic spacing of the nanoparticle, the dielectric properties and its local environmental conditions includes the substrate, adsorption and solvent [13].

- **Thermal properties**

  Comparing to the fluids in solid form, the metal nanoparticles have higher thermal conductivity. For example, the oxides such as alumina have thermal conductivity higher than that of water. So, fluid containing suspended solid particles are expected to display notable enhanced thermal conductivity compared to those of conventional heat transfer fluid [13].

- **Electric properties**

The dielectric properties, electrical transport and hall effect for nanomaterials differ from those for micron-sized materials due to increased interfacial atoms or ions and sinking of large amounts of defects at or near the grain boundaries. The electrical resistivity of nano crystalline metals is higher than that in both coarse grained polycrystalline metals and alloys. If crystal size is smaller than electron mean free path, grain boundary scattering dominates and hence electrical resistivity as well as the temperature coefficient is increased. The magnitude of electrical resistivity and hence the conductivity in composites can be changed by altering the size of the electrical conducting component [14].

- **Mechanical properties**

Mechanical properties of nanoparticles have novel applications in many fields such as surface engineering and nano manufacturing. Different mechanical parameters such as elastic modulus, hardness, stress and strain adhesion and friction can be surveyed to know the exact mechanical nature of nanoparticles. Besides these parameters surface coating, coagulation and lubrication also aid to mechanical properties of bulk material. Elastic constants of nano crystalline have been reduced considerably compared to those of bulk materials. This is due comparatively higher inter-atomic spacing in the boundary regions. The strength of nano crystalline materials increases considerably than that of coarse-grained materials. Hardness also increases with decreasing grain size in the conventional coarse grain materials. It is referred to as Hall Petch effect [15].

1.7.2 Chemical Properties

The reactivity of the nanoparticles with the target and stability and sensitivity to factors such as moisture, atmosphere, heat and light are the chemical properties that determine its applications. The nanoparticle's antibacterial, antifungal, disinfection, and toxicity properties make them suitable for biomedical and environmental usage; corrosive, anti-corrosive, oxidation, reduction and flammability characteristics of the nanoparticles determine their respective usage [9].

1.8 Synthesis method of Nanoparticles

1.8.1 Top-down approach

By this method, the nano-sized particles are obtained by the method of cutting or slicing the bulk material. Top-down synthesis techniques are extension of those that have been used for producing

micron-sized particles. This approach is inherently simpler and depend either on removal or division of bulk material or on the miniaturization of bulk fabrication processes to produce the desired structure with appropriate properties. The failure regarding this approach is the surface imperfection. For example, nanowires made by lithography are not smooth and may contain lot of impurities and structural defects on its surface. Examples of this techniques are high-energy wet ball milling, electron beam lithography, gas phase condensation, aerosol sprays, etc.

1.8.2 Bottom-up approach

Here, an assembly of smaller scale particles combined together to form a material which have dimension greater than from its beginning. It can be atom or molecule or cluster by cluster. Materials are built from molecular components which assemble themselves chemically by the principles of molecular recognition. The bottom-up has more advantages than the top-down approach because it has better chance of producing nanostructure with less defect better homogeneous chemical composition and good short and long ordering. Sol-gel synthesis, colloidal precipitation, hydrothermal synthesis, template assisted sol-gel synthesis, organo-metallic chemical route, reverse-micelle route, electro-deposition, etc. are some of the well-known bottom-up techniques for the preparation of nanoparticles [16].

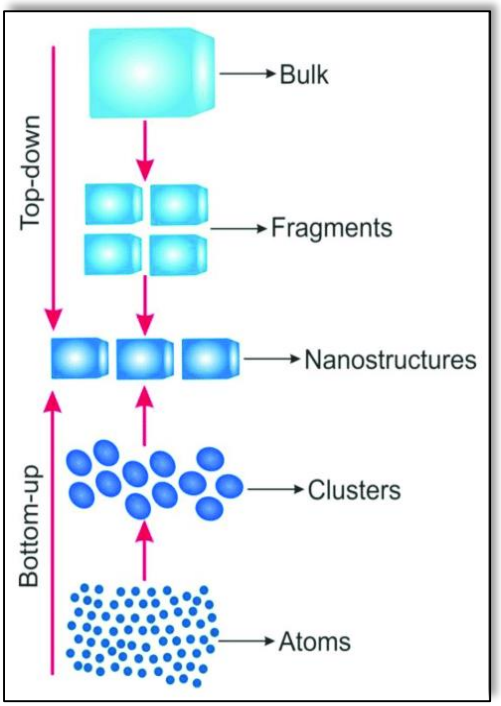

Figure.1.7 Illustration of top down and bottom up approach [16]

1.9 Nanoparticle Synthesis Classification

The synthesis of nanoparticle can be classified into liquid phase, gas phase and vapour phase methods:

(a) Liquid phase synthesis: This method involves wet chemical routes,

- Hydrothermal synthesis
- Co precipitation
- Sol Gel method
- Biometric synthesis
- Template synthesis
- Micro emulsion

(b) Gas phase synthesis: This method involves the vaporization of materials in a pressure of static inert gas. It can use solid or liquid or vapour.

Methods using solid precursors are:

- Pulsed laser ablation
- Ion sputtering
- Inert gas condensation

Methods using liquid or vapour precursors are:

- Chemical vapour synthesis
- Spray pyrolysis
- Thermal plasma synthesis

- Flame synthesis

(c) Vapour-phase synthesis

It is similar to liquid phase reaction. It is generally pursued at elevated temperature in vacuum. The vapour phase mixture is relatively unstable compared to the desired solid material. At a high temperature the vapour supersaturates. Once the nucleation occurs remaining super saturation is relieved by condensation or reaction of vapour phase molecules on the resulting particles. This initiate particle growth phase.

1.10 Hydrothermal method

The hydrothermal process involved mixing of precursors and proper agents into a solvent that enables the synthesis of a crystalline nanostructure with appropriate ratio. The procedure included transfers of the mixture into a sealed autoclave made of stainless steel lined with Teflon and heated in an oven at a specific temperature, time, and autogenous pressure [17]. Mostly, high pressure and temperatures are used in this method. When the container is heated, a high pressure is created in the container and the reaction takes place at this pressure is called hydrothermal reaction. The temperature and the amount of solution added to the autoclave determine the internal pressure produced. This method is used in the ceramic industry. After keeping it in the autoclaves for hours, it is taken out and filtered. After filtration obtained power is dried. In this way, nanoparticles can be synthesized by the hydrothermal method.

A large number of compounds have been synthesized under hydrothermal conditions. Hydrothermal synthesis is commonly used to grow synthetic quartz, gems, emeralds, rubies, and other single crystals. The method has proved to be efficient in the search for new compounds with specific physical properties. The techniques of crystallizing substances from high temperature non aqueous solutions at high vapour pressures are termed “solvothermal method”. The solvothermal synthesis method uses the organic solvents and super critical carbon dioxide. The hydrothermal technique is widely used for the preparation of various inorganic compounds, nanomaterials and zeolites. This technique is very popularly used by physicists, chemists, material scientists, engineers, and many others. This method is highly appreciated for the morphology control with purity of the product as compared to other conventional methods [18]. Hydrothermal method exploits the solubility of almost all inorganic substances in water at elevated temperature and

pressure subsequent crystallization of the dissolved material from the fluid. Water at elevated temperatures plays an essential role in the precursor materials transformation because the vapour pressure is much higher and the structure of water at elevated temperature is different from that at room temperature.

Disadvantages of the method include the need of expensive autoclaves, and impossibility of observing the crystal as it grows if a steel tube is used. There are autoclaves made out of thick walled glass, which can be used up to 300˚C and 10 bar [19].

Figure.1.8 Steel autoclave with Teflon liners

Figure.1.9 Hydrothermal oven used for synthesis

1.11 Nickel Oxide (NiO) Nanoparticles

Nickel Oxide, the chemical compound with formula NiO is one among the most important transition metal oxides with face centered cubic lattice structure used in all sort of application [20]. Bunsenite is the mineralogical form of Nickel oxide. NiO nanoparticles have brownish grey color. NiO nanoparticle is a composite semiconductor made of nickel and oxygen. Defects present in the structure of nickel oxide nanoparticle guides to non-stoichiometric nickel oxide which is good p-type semiconductor. Generally, the direct bandgap of NiO varies from 3.5-3.8 eV. The unique structure of NiO nanoparticle can be successfully utilized in the range of physical applications. They give superior magnetic, electrical, thermal, optical, catalytic and mechanical performance. Calcination process at 600˚C will generate crystalline NiO nanoparticles of high purity and single phase in nature. Nickel forms a series of mixed oxide compounds which are called nickelates. NiO adopts the NaCl structure with octahedral Ni^{2+} and O^{2-}sites [22]. The simple structure is commonly called rock salt structure. NiO nanoparticles have a rock salt crystal structure in its paramagnetic phase or ferromagnetic phase. In the catalytic field the rock salt crystal structure of NiO is used.

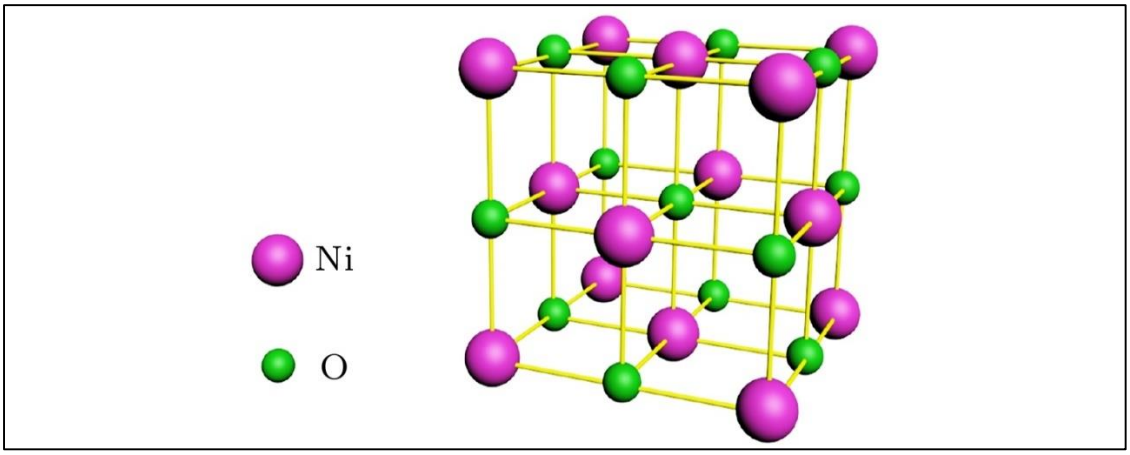

Figure.1.10 Structure of Nickel Oxide [21]

Like many other binary metal oxide, NiO is often non-stoichiometric meaning that the Ni to O ratio deviates from 1:1. In nickel oxide, this non-stoichiometry is accompanied by a color change with the stoichiometrically correct NiO being green and the non-stoichiometric NiO being black. We can prepare NiO using various methods. Upon heating above 400˚C, nickel powder reacts with oxygen to give NiO. The simplest and effective way is through pyrolysis of nickel compounds such as hydroxides, nitrates and carbonate which yields a light green powder. Synthesis from the

elements by heating the metal in oxygen can give it a grey color which indicate the non-stoichiometry [22].

Nickel oxide nanoparticles are graded as toxic. They can cause allergic reactions, prolonged harmful effects to aquatic life and possible damage to organs after exposure. It can also lead to cancer [22].

In NiO, 78.55% of nickel and 21.40% of oxygen are present. Molecular mass of NiO is 74.6928 g/m. Its density is found as 6.67 g/cm³. melting point is 2228 K. NiO is negligibly soluble in water. Magnetic susceptibility is $660.0\times 10^{-6}\ \mathrm{cm}^3/\mathrm{mol}$ and refractive index is 2.1818 [22]. NiO is one of very important catalysts in the field of chemical engineering. P-type semiconducting NiO is employed as a co-catalyst for photocatalytic water splitting. Porous NiO nanowire with high density of high index faced atom will have high catalytic efficiencies. NiO is an insulator both above and below the anti-ferromagnetic ordering temperature.

1.11.1 Applications of NiO

- In electrochromic coatings, plastics and textiles.
- In nanowires, nanofibers and specific alloy and catalytic applications.
- As a catalyst and anti- ferromagnetic layers.
- In light weight structural components in aerospace.
- Adhesive and coloring agents for enamels
- In active optical filters.
- In ceramic structures.
- In automotive rear- view mirrors and adjustable reflectance.
- In cathode materials for alkaline batteries.
- Energy efficient smart windows.
- P-type transparent conductive films.
- Materials for gas or temperature sensors.
- As a counter electrode.
- Energy storage: like many oxides nanoparticles, NiO offers extensive potential in the production of fuel cells and batteries. Specifically, it is of use in the production of cathodes in the preparation of other material components [23].

- As a photo catalyst

Photocatalysis

Dye pollutants play an important role in contaminating the aquatic eco-systems and are called ecological hazards in polluting the environment. But, about 15 % of the total world production of the dyes are lost to the effluents of the dying processes [24]. Nowadays, there is an increase in water scarcity due to this industrial wastes which turns as a threat to the public. This lead to a situation where International Environmental Standards become strict all over the world and new methods and technologies to remove organic dyes and other harmful pollutants. Combined methods like coagulation, electrochemical oxidation, coagulation flocculation, reverse osmosis and adsorption on activated carbon for this purpose however created more concentrated pollutant-containing phase. Amongst upcoming chemical treatments, recent developments in oxidative degradation of organic compounds led to a process called "advanced oxidation processes", where at times, heterogeneous photo catalysis is employed to degrade a majority of the organic pollutants.

Photo catalysis is defined as a "photo-induced" reaction where we use a catalyst to speed up the reaction. This reaction starts with absorption of a photon with sufficient energy, equals or greater than the band-gap energy (E_g) of the catalyst. Absorption of these photons produce electron–hole pairs on the surface of catalyst which reduce or oxidize the organic materials present in aqueous solutions. The prime advantage of applying this technique is its ability to convert the organic pollutants into non-toxic species (CO_2, H_2O) and further separation processes are not needed [24].

NiO is used for this purpose due to their exceptional catalytic activity and greater stability. NiO is a p-type semiconductor with a wider band gap between valence and conduction band, which make it a good photo catalyst [25]. Here, I am going to evaluate the photo catalysis dye degradation efficiency of hydrothermally synthesized NiO nanoparticle under natural sunlight by taking Rhodamine B (RhB) as model dye.

CHAPTER 2

LITERATURE REVIEW

Ganachari *et al.* [26] prepared NiO nanoparticles by self-propagating low temperature combustion process using the nickel salt and polyethylene glycol as fuel. The precursors were nickel sulphate, oxalic acid, polyethylene glycol. Nickel oxalate is then prepared by dissolving equi molar quantity of Nickel sulphate heptahydrate and Oxalic acid in small amount of demineralized water. Light green precipitate of nickel oxalate thus formed turned powdery grey color when calcined at temperature of about 700˚C. The thermal decomposition of nickel oxalate resulted in NiO with high surface area. Self-propagating low temperature combustion process is good way to produce high quality nano-sized Nickel oxide powder.

Nguyen *et al.* [27] performed a comparative study on electro-chemical performance of nano porous nickel oxide(NiO), nano sheets and nano wires. The advanced nano porous NiO NP were synthesized by a facile hydrothermal method followed by thermal calcination. The synthesized materials are characterized by SEM, XRD, nitrogen adsorption/ desorption isotherms and demonstrated the nano porosity and crystallinity of NiO nano sheets and wires. The results showed that the nano porous NiO nano sheets possessed a higher current density than that of nanowires by ten times.

Kumar *et al*. [28] synthesized pure and 5 mol % Eu doped Nickel oxide (NiO) by microwave assisted hydrothermal process. The phase and purity of synthesized NiO nanoparticles were confirmed from XRD and Rietveld refinement analysis. SEM analysis revealed that the un-doped nanoparticle is porous flake-like structures while the doped samples were found aggregated. XPS analysis showed that Eu doping increase concentration of holes, $Ni^{2\cdot}$ vacancies and defective oxygen concentration in the nanoparticle. On doping with Eu, the ferromagnetic behavior increases due to increased oxygen defects and uncompensated surface spins. Raman spectroscopy investigation shows the absence of 2 M vibrational mode and reduced anti-ferromagnetic coupling in the prepared samples. It also substantiated the presence of defects in the prepared samples. Eu doping produced local vibrations which overlap with SO mode of Nickel oxide and shifting of 1 M band due to its higher mass. Magnetic properties of NiO is modified by addition of Eu dopant.

Xueliang Li *et al*. [29] prepared NiO nanoparticles by thermal decomposition of nickel dimethylglyoximate. Rod like nickel dimethylglyoximate precursor is prepared from dimethylglyoxime and $NiSO_4$ under magnetic stirring for 1h. Red flocculates of nickel dimethylglyoximate were filtered, washed and was heated to 400˚C at heating rate of 5˚C mm^{-1} and calcining at 400˚C for 2h. Thermal gravimetric analysis was done to study the thermal behaviour of obtained nickel dimethyl glyoximate and the curve showed that it starts to decompose at about 255˚C. The major weight loss happened between 300˚C and 385˚C. The total weight loss is ~ 25.51% which was close to theoretical value. The reaction was completed by 385˚C and thus 400˚C was chosen as the calcining temperature. XRD pattern showed cubic crystalline NiO structure with no impurity or other precursors. Average size was calculated by Debye - Scherrer formula. TEM images nickel dimethylglyoximate precursor displayed rod-like morphology. The average particle size was consistent with XRD result. SAED patterns recorded were same and diffraction rings matches the X-ray Diffraction peaks, which indicates that the nanoparticles are polycrystalline. The calcining time and temperature have less effect on the morphology of synthesized nanoparticle. The optical absorption band gap of NiO nanoparticles was found to be 3.51e V.

Sabouri *et al*. [30] synthesized Nickel oxide nanoparticles by green co- precipitation method using Nickel nitrate hexahydrate and starch as Ni precursor and capping agent. Ammonia is also applied as a complex agent. Band gap of NiO is calculated about 3.55 e V. They tested NiO as a photo catalyst for the degradation of MB under UV light for 270 minutes. 80% of dye is degraded in the presence of NiO. Diffraction pattern showed that the synthesized sample possess FCC crystalline structure of NiO. Because of degradation of methylene blue NiO is an effective photocatalyst in waste treatment.

Jeba *et al.* [31] prepared NiO nanoparticles through biological green method, one of the cheapest method. They synthesized nanoparticles from pisonia alba leaf extract. Extract containing biomolecules can act as a capping agent. By using XRD, TEM, EDAX and UV, structural and optical properties of catalyst is studied. Photocatalytic degradation of methylene blue dye is done using the NiO nanoparticles and it is evident that the degradation of dye increases with increasing

in concentration of photocatalysts. TEM and SAED pattern confirmed the formation of the NiO nanoparticles. The particle size varied from 10-14 nm. XRD and SAED pattern showed the crystalline nature of synthesized samples. They reported 77.7% catalytic efficiency for the degradation of methylene blue in 60 minutes at 500W intensity of light.

Kayani *et al*. [32] prepared nickel oxide nanoparticles by sol-gel method using Ammonium hydroxide and Nickel nitrate as precursors. The NiO nanoparticles were annealed at temperature 400˚C and 1000˚C. Later, nanoparticles were characterized by XRD, FT IR, VSM. The XRD results showed that NiO nanoparticles have good nano crystalline hexagonal structure. their grain size also had an increase from 12.4nm to 20.7nm with increase in annealing from 400˚C to 1000˚C. Their optical studies revealed that they have low absorbance in the IR and Visible region with a band gap of 3.02eV at 400˚C. This band gap is increased to 3.14eV at 1000˚C. This is due to the increase in the defect level.

Danial *et al*. [33] prepared nanoparticles by sol-gel method and their electro catalytic activity studied at various condition. The prepared nanoparticles were annealed at different temperature such as 200˚C, 400˚C and 600˚C and anchored on a glassy carbon(GC) electrode. FE SEM, TEM, and XRD were taken. It is seen that nano NiO_x /GC was used for glucose electro oxidation.

Shamim *et al*. [34] prepared NiO nanoparticles by sol-gel method using Nickel (ii) nitrate hexahydrate and 0.5 M sodium hydroxide as precursor. XRD, SEM and EDX of sample were taken. From the results, it is understood that the NiO nanoparticles were made without any impurity. The morphological study showed nano range of particle and elemental analysis traced Ni and O elements.

Usha *et al*. [35] deposited NiO thin films on a degreased glass substrates by rf magnetron sputtering at room temperature using 99.99% pure NiO target. Ultra-pure Argon gas were introduced into the chamber. The rf power was varied as 100, 150 and 200 W. The thickness of the film was measured. The structural properties of NiO thin films were studied using XRD and found that films have a cubic structure with preferential growth along (200) orientation. The rf power induced changes in optical properties of NiO films were studied. The rf power induced grain growth, reduction in dislocation density, and strain were evaluated from XRD study. The maximum transmittance of 95% was observed for the film deposited at 100 W rf power. A systematic reduction in the optical

band gap is observed with increasing rf power. As the rf power increases, refractive index and extinction coefficient value also increase.

Zorkipli *et al*. [36] synthesized NiO nanoparticles through sol gel method using Nickel(ii) nitrate hexahydrate dissolved in 20 ml isopropanol and 20 ml polyethylene glycol. The solution was controlled at a pH 11 and the calcination temperature at 450˚C. Phase identification and structural analysis were performed by XRD. A cubic structure was formed in the NiO nanoparticles. The NiO nanoparticles were formed without any impurity. The morphological analysis was demonstrated in a nanoscale range, and Ni and O elements were successfully traced.

Alagiri *et al*. [37] synthesized nickel oxide nanoparticles in the presence of agarose polysaccharide by sol gel method. Its structural, morphological, optical and magnetic properties were examined by XRD, TEM, UV –Visible spectroscopy and Superconducting quantum interference device magnetometer. The result of thermo gravimetric analysis of the precursor product showed that the proper calcination temperature was at 400˚C. XRD result revealed that the obtained product was nickel oxide with FCC structure. TEM image demonstrated that the nickel oxide nanoparticles have spherical shape with size around 3nm. Analysis of FTIR spectra confirmed the composition of product. The optical absorption band gap of NiO nanoparticles was found to be 3.15eV.

Jayakumar *et al*. [38] prepared NiO nanoparticles by co precipitation method using nickel nitrate as precursor and sodium hydroxide as precipitating agent. The synthesized nanoparticles were studied by powder XRD. FESEM, EDAX and FTIR. The XRD pattern exhibit face centered cubic phases for the synthesized NiO nanoparticles. FESEM images showed that the NiO nanoparticles have oval shaped morphology. The formation of NiO nanoparticles was confirmed from EDAX and FTIR analysis. The amount of different elements present in the synthesized sample are estimated and found to be nearly stoichiometric. The NiO nanoparticles were used as photocatalyst for the degradation of Methylene Blue dye from aqueous medium. The absorption spectra clearly showed that when exposed to solar radiation the degradation of M B dye from aqueous medium increases as the reaction time increases. This results indicate that NiO nanoparticle act as a photocatalyst in the degradation of MB from aqueous medium.

Mohammadyani *et al*. [39] produced nickel oxide nanoparticles via rapid Microwave assisted method. $Ni(OH)_2$ precursor was obtained by slow drop wise addition of 0.1M sodium hydroxide to 0.1M nickel nitrate. The precipitate formed is then dried at 320˚C to form NiO nano powder.

XRD analysis showed that this substance is a typical α- type nickel hydroxide powder. All of the diffraction peaks were broad. The XRD pattern indicated “saw-tooth” reflection. TEM images showed that the NiO nanoparticles have mean crystallite size of 30nm. Both SEM and TEM morphologies indicate that the primary nanoparticle is clustered together to for larger agglomerates. Morphology of produced nano powder showed NaCl type cubic structure. Color alteration was recognized during NiO formation. This is attributed to the non- stoichiometric characters of nanoparticles.

Teoh *et al*. [40] prepared NiO nanoparticles by sol-gel method using poly black copolymer as the surfactant and $Ni(NO_3)_2.6H_2O$ as the inorganic material. They studied the effect of calcination temperature and the concentration of water on NiO characteristics and observed that the NiO properties can be varied by the proper tuning of growth parameters. XRD analysis showed the formation of pure NiO at a calcine temperature of 923K. When the concentration of water is increased, the oxidation process of the metallic Ni to form the NiO is reduced. But it would not affect the structural type of NiO nanoparticles. The thermal stability of NiO nanoparticles are found to enhanced with the use of copolymer as surfactant. They showed that high surface area of NiO nanoparticles can be obtained by calcining the samples at low temperature.

CHAPTER 3

CHARACTERIZATION TECHNIQUES

3.1 X-Ray Diffraction Spectroscopy

X- ray diffraction(XRD) is an important non- destructive technique used to study the crystal structures and atomic spacing by analyzing all kinds of matter ranging from fluids to powders and crystals. In 1912, a German physicist von Laue reasoned that if crystals were composed of regularly spaced atoms which might act as scattering centers for X-rays, and if X-rays were electromagnetic waves of wavelength equal to the interatomic distance in crystals, then it should be possible to diffract X-rays using crystals [41].

Bragg provided an alternative explanation for the measurement of diffraction of monochromatic X-ray from single crystals after Laue discovered of X-ray diffraction. He assumed that crystals are in layers or atomic planes (lattice planes-hkl) with spacing, d. When X-ray beams fall on the atoms or molecules of a crystal lattice, they get scattered. At certain incident angles of the X-ray beams, the scattered X-rays interfere constructively and a diffraction pattern is produced. According to Bragg's law, the scattered X-rays will interfere constructively only if the path difference between the beams is an integral multiple of the wavelength of the X- rays.

Bragg's law is expressed as,

$$n\lambda = 2d\ sin\theta$$

where n is the order of diffraction, λ is the wavelength of the incident X-rays, d is the inter planar spacing and θ is the diffraction angle.

The X-ray diffractometer consists of three basic elements. An X-ray tube, a sample holder and an X-ray detector. X-rays are generated in a cathode ray tube by heating a filament to produce electrons which are accelerated towards the target by applying a voltage and bombarding the target material with the electrons. Characteristic X-rays are emitted when electrons have enough energy to dislodge the inner shell electrons. This X-ray signal is recorded and processed by a detector, which then converts it to a count rate, which is then sent to a system like a printer or a computer monitor as output.

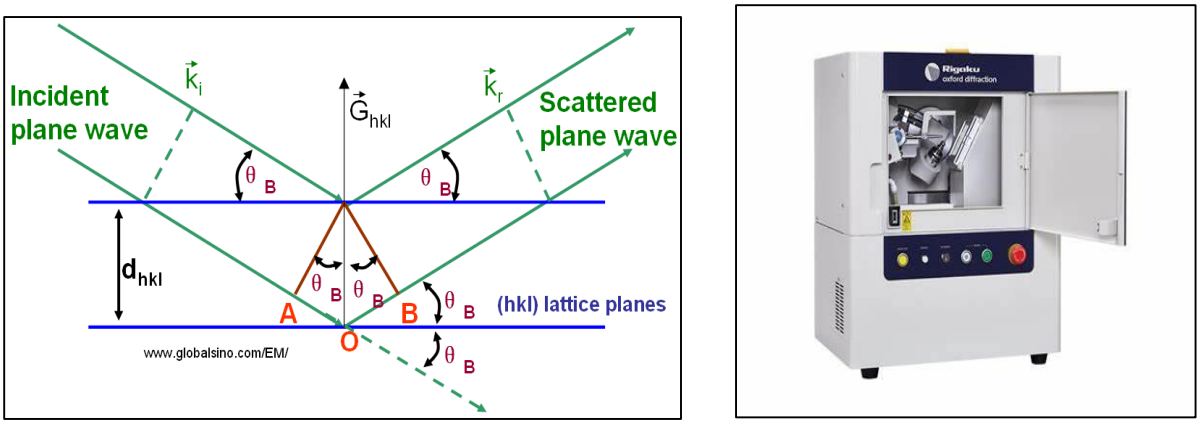

(a) (b)

Figure.3.1 Schematics of X- Ray diffraction pattern (b) X- Ray Diffractometer

3.1.1 Experimental Techniques

The experimental techniques used in collecting X-ray diffraction data are the rotating-crystal method, the Laue method, and the powder method. Regardless of the method used, the quantities measured are essentially the same.

i. The scattering angle 2θ between the diffracted and the incident beams i.e., the X-ray detector collects the diffracted X-rays by rotating at an angle of 2θ from which one can find θ. The inter planar spacing, as well as the orientation of the plane responsible for the diffraction, can be determined by substituting sin θ into Bragg's law.

ii. The intensity I of the diffracted beam determines the cell structure F_{hkl} and hence gives the information concerning the arrangement of atoms in the unit cell [42].

The Rigaku Miniflex 600 is a multipurpose powder diffraction instrument that can be used for phase identification, phase quantification, crystallite size, strain, lattice parameter refinement, Rietveld refinement, molecular structure and percentage crystallinity. The powder method is the most convenient and quickest method for obtaining the diffraction data and is applicable even if the specimen is not a single crystal. The sample may be fine-grained powder or it may be polycrystalline. A monochromatic beam impinges on the specimen, and the diffracted beams are recorded on a cylindrical film surrounding it.

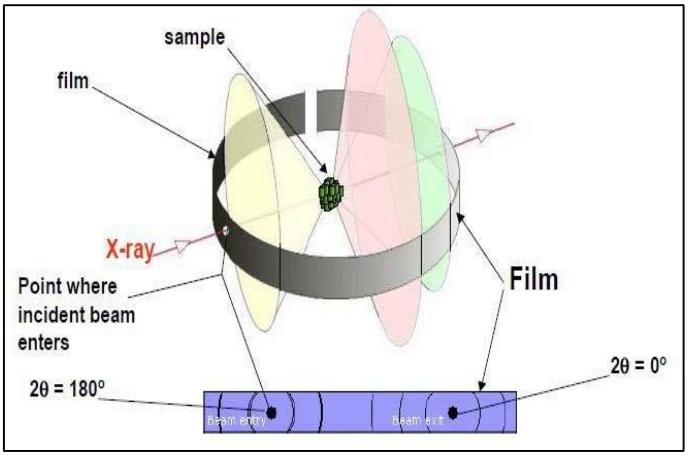

Figure.3.2 Schematic representation of the powder method and X-ray powder diffraction pattern

3.2 UV-Visible Spectroscopy

UV-Visible spectroscopy is a useful technique for the identification and analysis of both organic and inorganic compounds by detecting the absorptivity or reflectance of a sample under ultra-violet to visible light wavelength range. Here, the sample is exposed to a beam of light ranging from 200-1100 nm where the sample absorbs the light and the transmitted light is measured by a detector. It measures the transition of π-electrons in molecules from their ground state to excited states. The analytical information can be revealed in terms of transmittance, absorbance or reflectance of energy.

This technique is based on the Beer-Lambert principle which states that the quantity of light absorbed by a substance dissolved in a fully transmitting solution is directly proportional to the concentration of the substance and the path length of the light through the solution when the wavelength of the incident light remains fixed.

$$A = \in dc = log \frac{I_0}{I}$$

where 'A' is the absorbance, 'ϵ' is the molar absorptivity ($Lmol^{-1} cm^{-1}$), 'd' is the path length of the cuvette containing the solution (cm), 'c' is the concentration of the compound in the solution ($mol\ L^{-1}$), I_0 and I are intensity of the incident and the transmitted light respectively.

UV-Visible spectrophotometer consists of a light source, sample holder and a monochromator. The radiation source is often a tungsten filament, deuterium arc lamp, xenon arc lamp or light emitting diodes for the visible wavelengths. The monochromator works as a diffraction grating or

prism to disperse the beam of light into the various wavelengths. There are two types of spectrophotometers: single beam and double beam. In a single beam instrument, all the light is made to pass through the sample cell. In a double beam instrument, light from the source is split into two beams before it reaches the sample. One beam i.e., the sample beam passes through the cuvette containing a solution of the compound being studied in a transparent solvent. The other one i.e., the reference beam passes through the cuvette containing only the solvent. The detector measures the intensity of light transmitted from the cuvette. The sample handling is done with the help of cuvette which is an optically transparent cell that holds the material under study.

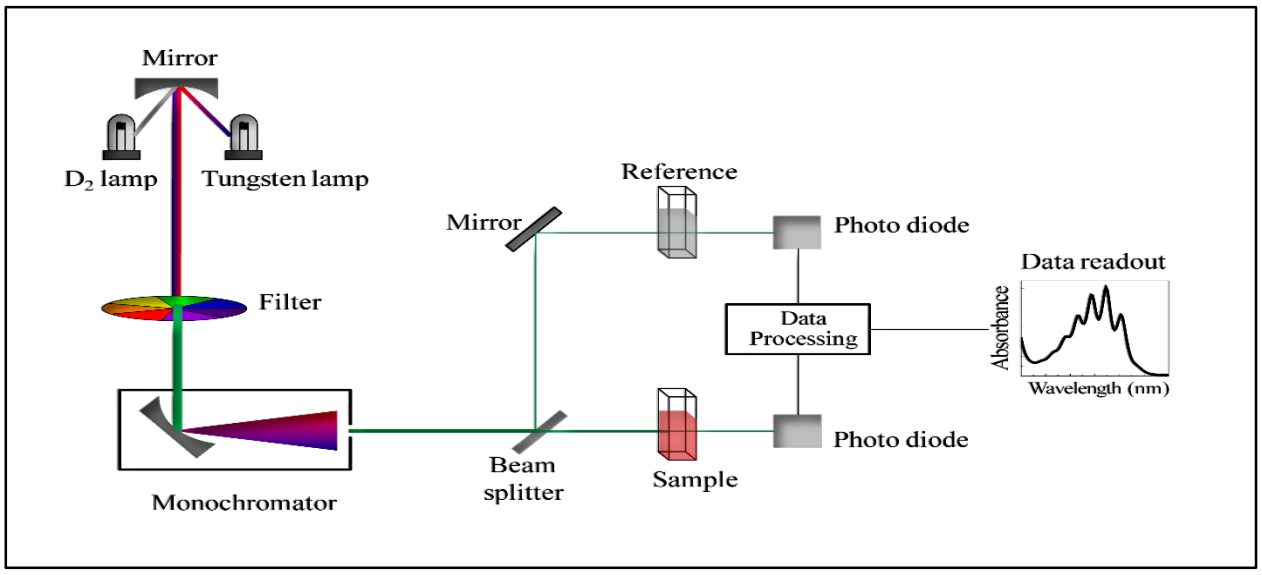

(a)

(b)

Figure.3.3 (a)Working principle UV- Visible spectroscopy (b) UV-Vis spectrophotometer

The absorption studies of the sample were done using the Jasco V-760 spectrophotometer. It is a high resolution UV-Visible double beam spectrophotometer with double monochromator for

exceptional stray light and absorbance linearity, variable spectral bandwidth and photomultiplier tube detector. The light sources used in this spectrophotometer are the halogen lamp and deuterium lamp with wavelength ranging from 187-900 nm. It provides excellent sensitivity for diffuse reflectance or transmittance of solid and liquid samples using an integrating sphere.

3.2.1 Determination of optical band gap

The band gap energy of a nanoparticle is estimated from Tauc plot using the equation,

$$(\alpha h\vartheta)^{\frac{1}{n}} = C\ (h\vartheta - E_g)$$

where 'α', 'ϑ', 'C', and 'E_g' are the molar absorption coefficient, frequency of light, an arbitrary constant and the band gap of the nanoparticles respectively and n is the power factor of the transition mode which dependent upon the nature of material. The value of exponent denotes the nature of the electronic transition, whether allowed or forbidden and whether direct or indirect.

For direct allowed transitions: n = ½

For direct forbidden transitions: n= 3/2

For indirect allowed transitions: n = 2

For indirect forbidden transitions: n = 3

Typically, the allowed translations dominate the basic absorption processes, giving either n=1/2or n=2 for direct and indirect transitions respectively.

The plotting of $(\alpha h\vartheta)^{1/n}$ versus the photon energy ($h\vartheta$) gives a straight line in a certain region. The extrapolation of this straight line will intercept the ($h\vartheta$) axis to give the value of the optical energy gap (E_g) [43].

3.3 Scanning Electron Microscopy (SEM)

Scanning Electron Microscope (SEM) uses a focused beam of high energy electrons to generate a variety of signals at the surface of solid specimen. The signals that derive from electron- sample interaction reveal information about the sample including external morphology (texture), chemical composition, and crystalline structure and orientation of materials making up the sample. In most applications, data are collected over a selected area of the surface sample, and a 2-dimensional

image is generated that displays spatial variations in these properties. Areas ranging from approximately 1 cm to 5 microns in width can be imaged in a scanning mode using conventional SEM techniques (magnification ranging from 20X to approximately 30,000X, spatial resolution of 50 to 100 nm). The SEM is also capable of performing analyses of selected point location on the sample; this approach is especially useful in qualitatively or semi- quantitatively determining chemical compositions (using EDS), crystalline structure, and crystal orientations (using EBSD). The design and function of the SEM is very similar to the EPMA and considerable overlap in capabilities exist between the two instruments [44].

3.3.1 Principle

Accelerated electrons in a SEM carry significant amounts of kinetic energy and this energy is dissipated as a variety of signals produced by electron- sample interactions when the incident electrons are decelerated in the solid sample. These signals include secondary electrons (that produce SEM images), backscattered electrons(BSE), diffracted backscattered electrons that are used to determines crystal structures and orientations of minerals), photons (characteristics X-rays that are used for elemental analysis and continuum X rays), visible light (cathodoluminescence) and heat. Secondary electrons and backscattered electrons are commonly used for imaging samples: secondary electrons are most valuable for showing morphology and topography on samples and backscattered electrons are most valuable for illustrating contrasts in composition in multiphase samples (i.e., for rapid phase discrimination). X-ray generation is produced by inelastic collision of the incident electrons with electrons in the discrete orbitals (shells) of atoms in the sample. As the excited electrons return to lower energy states, they yield X -rays that are of a fixed wavelength. Thus the characteristic X- rays are produced for each element in a mineral that is "excited" by the electron beam. SEM analysis is considered to be "non-destructive"; that is X rays generated by electron interactions do not lead to volume loss of the sample, so it is possible to analyze the same materials repeatedly [44].

Essential components of all SEMs include the following:

- Electron Source ("Gun")
- Electron Lenses
- Sample Stage

- Detectors for all signals of interest
- Display/Data output devices
- Infrastructure requirements:

    Power supply

    Vacuum System

    Cooling system

    Vibration-free floor

    Room free of ambient magnetic and electric fields

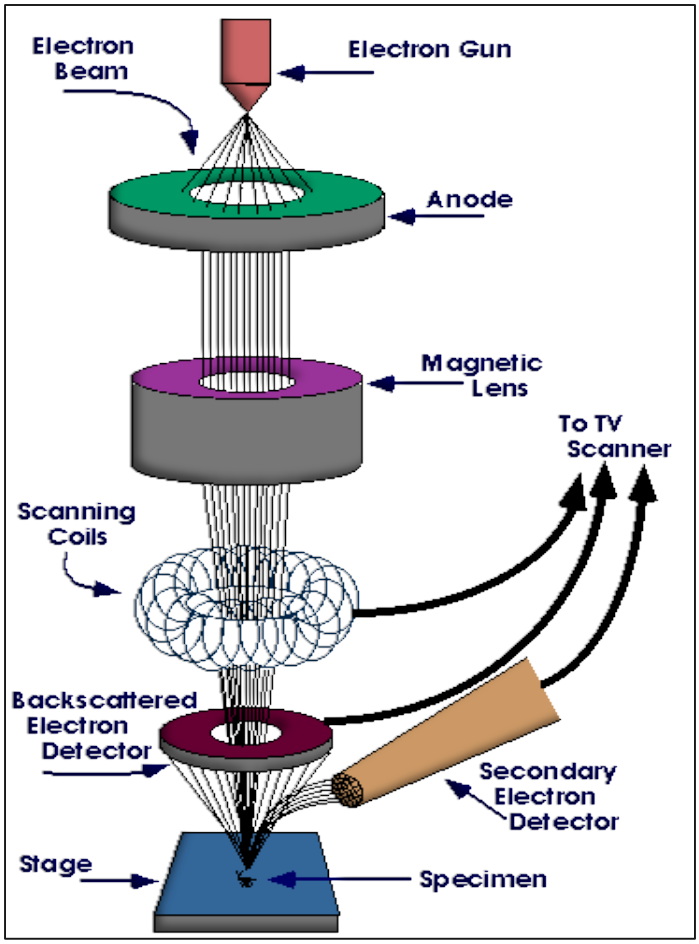

Figure.3.4 Typical diagram of SEM

3.3.2 Working

The SEM is an instrument that produces a largely magnified image by using electrons instead of light to form an image. A beam of electron is produced at the top of microscope by an electron gun. The electron beam follows a vertical path through the microscope, which is held within a vacuum. The beam travels through electromagnetic fields and lenses, which focus the beam down toward the sample. Once the beam hits the sample, electrons and X-rays are ejected from the sample.

Detectors collect these X-rays, backscattered electrons and secondary electrons and convert them into a signal that is sent to a screen similar to a television screen and this produces a final image [45].

3.3.3 Applications

The SEM is routinely used to generate high-resolution images of shapes of objects and to show spatial variation in chemical composition:

- Acquiring elemental maps or spot chemical analyses using EDS.
- Discrimination of phases based on mean atomic number using BSE.
- Compositional maps based on differences in trace element “activators” using CL.
- The SEM is also widely used to identify phases based on qualitative chemical analysis and/ or crystalline structure [45].

CHAPTER 4

MATERIALS AND METHODS

4.1 Materials used

Nickel nitrate $Ni(NO_3)_2.6H_2O$ and Sodium hydroxide (NaOH), distilled water.

4.2 Experimental Methods

Preparation of NiO

The nickel oxide nanostructure was prepared by hydrothermal method using Nickel nitrate ($Ni(NO_3)_2.6H_2O$ and Sodium hydroxide (NaOH) as precursors. 1M nickel nitrate solution is prepared in 40 mL DI water and 0.7M NaOH is added to it. After a continuous stirring for 30 minute, the final solution is transferred to a Teflon-lined beaker which is placed in the autoclave, in the hydrothermal oven at 180˚C for 24 hours. After the oven cools down, the autoclave is unsealed and the produced $Ni(OH)_2$ solution is poured into a funnel lined with filter paper to drain all the precipitates. The resulting product is thus filtered, washed with DI water and absolute ethanol and finally dried in hot air oven at 60˚C overnight. It is then calcined at 500˚C for 3 hours to produce Nickel oxide.

Photocatalysis

50 mg of NiO nanoparticles were added into 10 ppm solution of Rhodamine B (RhB) dye and is stirred at dark condition to evaluate adsorption property. In order to study photocatalytic activity, the solution was exposed to sunlight after attaining the adsorption-desorption equilibrium. Then we took the UV spectrum in regular intervals of 15 min.

The photocatalytic dye degradation of Rhodamine B dye using NiO as photocatalyst can be calculated from the equation

$$\textbf{\% of degradation} = \frac{(C_0 - C_e)}{C_0} \times 100$$

Where C_0 is the initial concentration of the dye and C_e is the final concentration of the dye after irradiation [46]

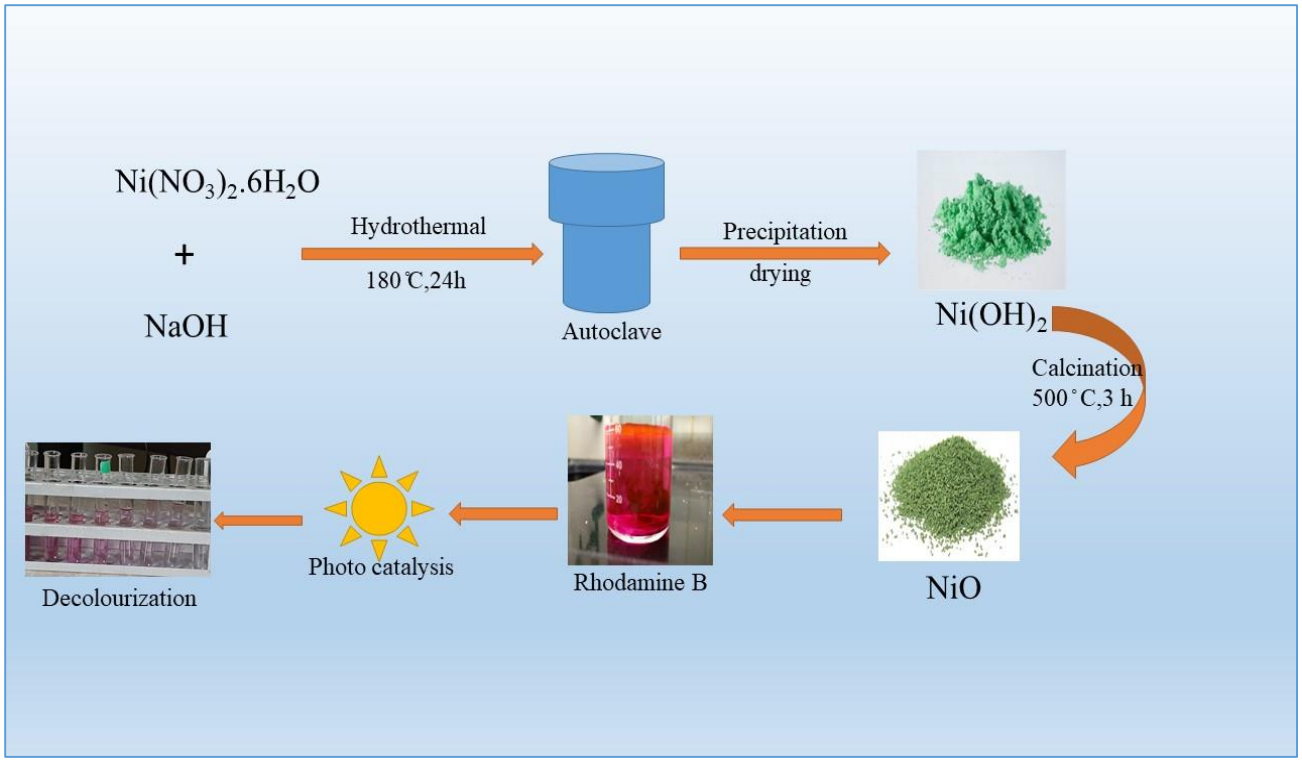

Figure.4.1 Schematic diagram of experimental procedure

CHAPTER 5

RESULT AND DISCUSSION

5.1 X-ray Diffraction analysis

XRD spectrum of NiO nanoparticles synthesized at 180˚C in 2θ range of 30˚to 80˚using CuKα radiation (λ=0.1504 nm) was shown in Figure.5.1. The diffraction peaks in the spectra are in agreement with the reported JCPDS data (file card no. 47-1049) [47]. The synthesized sample shows diffraction peaks at 2θ =37.10˚, 43.30˚, 62.87˚, 76.50˚, 79.22˚corresponding to crystal planes (111), (200), (220), (311) and (222) which attributes to the face centered cubic structure (FCC) of NiO with a space group of F m-3m. The comparatively intense peak reflects a moderate crystalline size. No other peaks related to impurities are found. Unit cell parameters and lattice constants are confirmed by identification of the phases using QualX software [48].

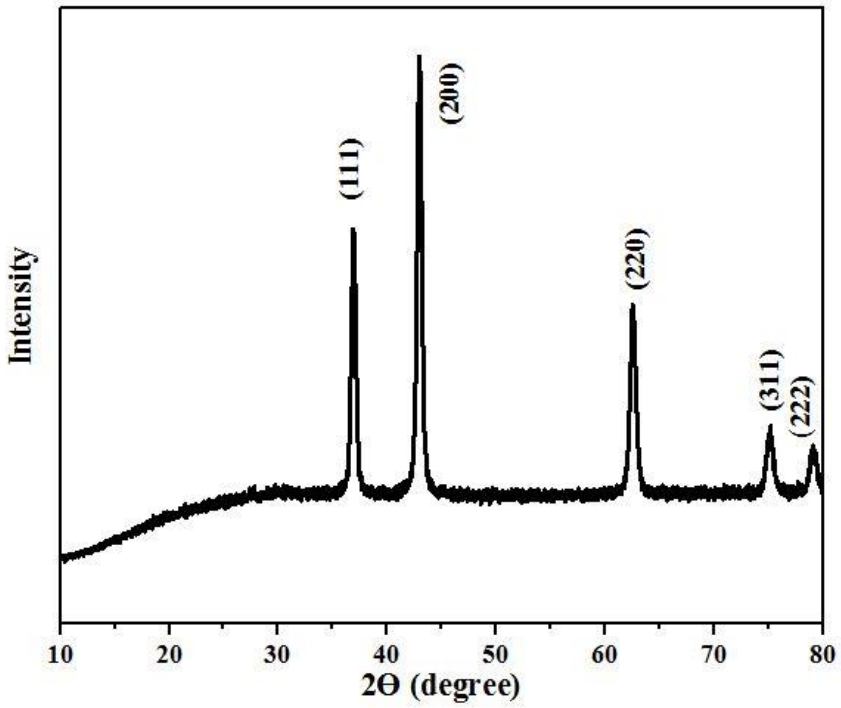

Figure.5.1 XRD pattern of NiO nanostructures

Rietveld Refinement technique using Crystallographic Open Database(COD) as input file was used to establish the final structures [48]. The appropriate values of the goodness of fit parameters

such as Rp (profile), R_{wp} (weight profile), R_e (expected) and χ^2 values of NiO sample are given in Table 5.1

Table 5.1 Lattice parameters of NiO by refinement

Sample code	Rp	R_{wp}	R_e	χ^2	a (Å)	b (Å)	c(Å)	V(Å^3)	Crystallite size	c/a
NiO	27	16.4	13.9	1.32	4.17	4.17	4.17	72.74	17.88	1

Crystallite size of the prepared NiO nanostructures are calculated by Debye-Scherrer formula [48] given as

$$\boldsymbol{D = \frac{k\lambda}{\beta \cos\theta} = \frac{0.89\,\lambda}{\beta \cos\theta}}$$

Where, β represent the integral half width, k represent a constant called shape factor, λ is the wavelength of CuKα source radiation (01540 nm), and D corresponds to the crystallite size and θ is the Bragg angle. From this equation we found that the crystallite size of the prepared NiO nanostructure is about 17.88 nm.

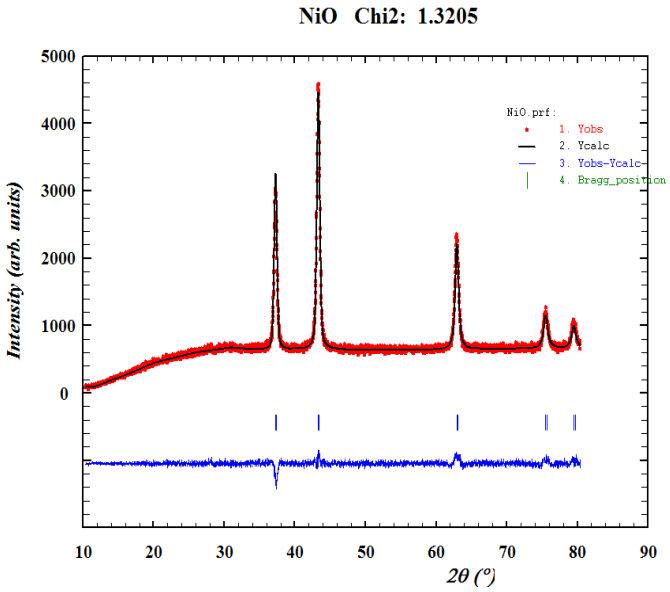

Figure.5.2 Refinement patterns of NiO

5.2 UV-Visible Spectroscopy

The optical properties of hydrothermally synthesized NiO nanoparticles were studied using Jasco-V 760 spectrophotometer. The Figure.5.3 shows UV-Visible reflectance spectrum of the sample recorded in the range of 200-800 nm.

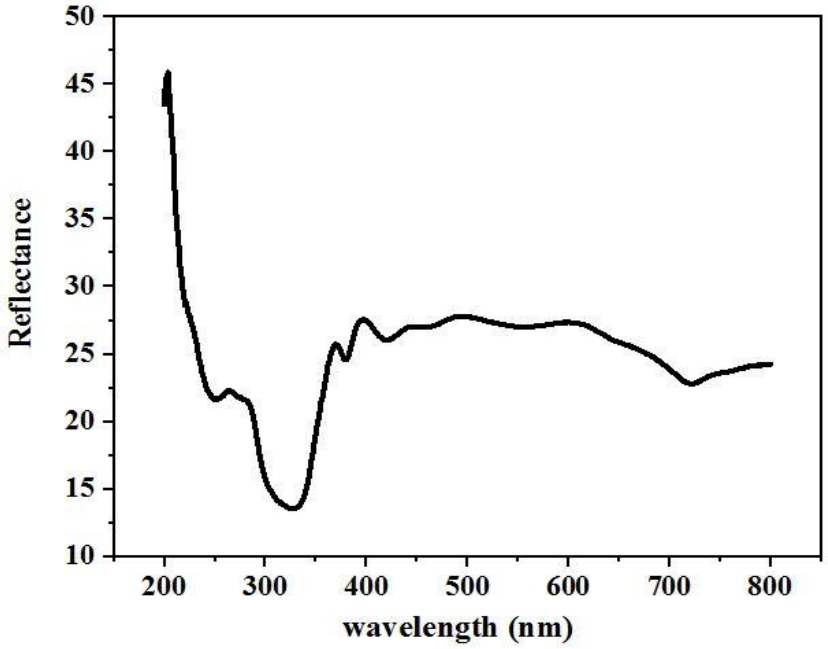

Figure.5.3 UV-Visible reflectance spectrum of NiO

5.2.1 Determination of optical bandgap- "Tauc plot"

Bandgap is one of the important parameter that deals with material properties. By Diffuse Reflectance Spectrum, the bandgap Eg of the synthesized particles were determined by Tauc plot method by calculating Kubelka-Munk function [48]. The optical bandgap of synthesized NiO nanoparticles was estimated by the shoulder peak of the spectra that corresponds to the fundamental absorption edges in the samples. Using Kubelka –Munk function, we could find the absorption of the sample and is given by,

$$\alpha = \frac{(1-R)^2}{2R} = k/s$$

Where R is the reflection coefficient, k is the absorption coefficient and s is the scattering coefficient. The tauc plot equation is [43]

$$(\alpha h\vartheta)^{\frac{1}{n}} = C\ (h\vartheta - E_g)$$

Where C is a constant which is independent of energy, h is Planck's constant, ϑ is the frequency of incident photon, E_g is the optical bandgap energy of the nanomaterial and 'n' is called the power factor. It is clear from above equation that the fundamental energy band gap always depends on the variation in optical absorption coefficient [35]. Depending upon the nature of transition, n can have values $1/2$, $3/2$, 2 or 3 for direct allowed, direct forbidden, indirect allowed, and indirect forbidden transition respectively. In this case, the value of n is ½ due to the direct bandgap feature of NiO. We can find the band gap energy of NiO nanoparticles from the intercept of extrapolated linear fit for plotted data versus the $h\vartheta$ as shown in Figure.5.4.

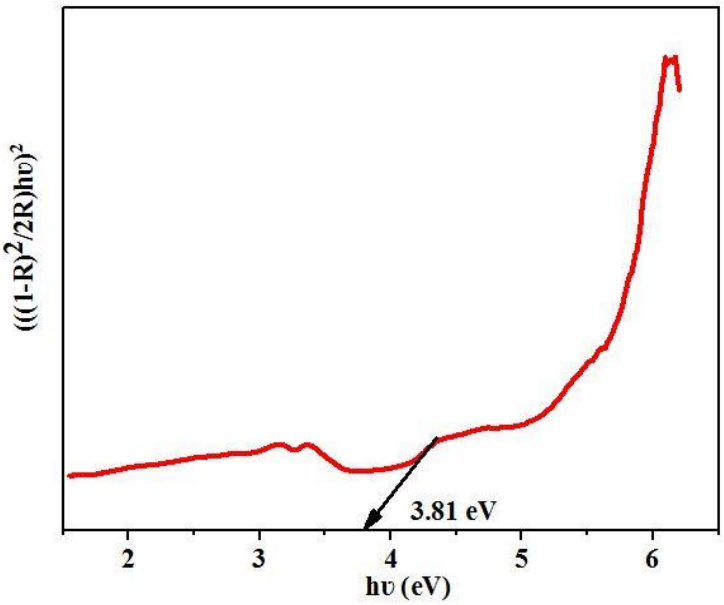

Figure.5.4 Tauc plot of NiO nanoparticles

Among different metal oxides, NiO nanoparticles are p-type semiconductors with a wide band gap of about 3.6eV [49]. The optical reflectance intensity is found at about 330 nm (3.75 eV) [47]. The bandgap value, E_g that we calculate from the Tauc plot is 3.8 eV. The increase in the bandgap occurs when the size of particle decrease due to the confinement of electrons and holes as compared with the reported papers [50]. Nickel oxide nanoparticles are semiconducting with a direct transition at this energy.

5.3 Morphological Analysis

Morphology properties of hydrothermally synthesized NiO nanoparticles are analyzed using FESEM.

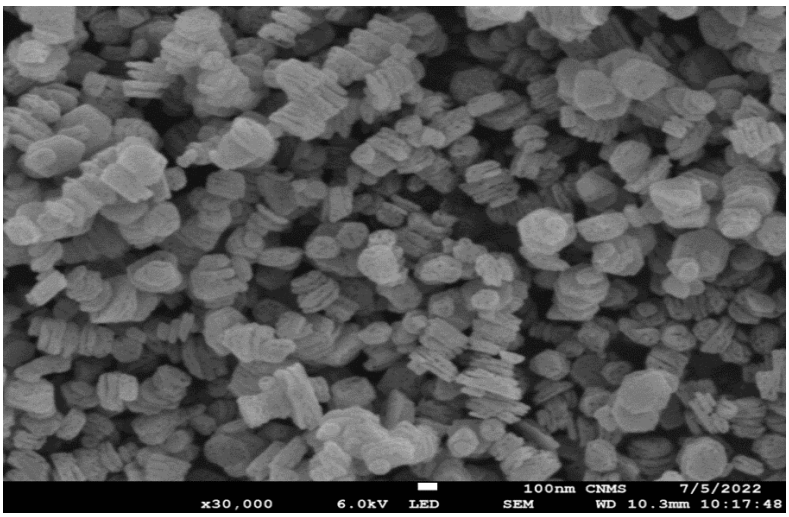

Figure.5.5 SEM images of synthesized NiO

NiO nanoparticles possess an oval shaped morphology without any agglomeration. Uniformity obtained in FESEM images reveals that the hydrothermal synthesis at 180˚C for 24h is an accurate route for the preparation of NiO. As compared with other low temperature hydrothermal route the procedure [27] we followed at 180˚C is producing the defined morphology for the application based on NiO.

5.4 Photocatalytic Study

Environmental problems associated with textile and paper industry is that the waste water effluents contain large amount of hazardous pollutants like aromatic compounds and organic dye and these are very harmful to aquatic eco-system. In order to degrade this toxic dyes, we need a suitable method for the removal of this and to control environmental and water pollution. Among this, photo catalysis is considered to be an important oxidation method for the degradation of industrial dyes. Parameters like band gap, size and defects in nanoparticles are influence the efficiency of the photo degradation process [48]. Here in the present study we are going to evaluate the photo

catalytic dye degradation efficiency of our NiO nanoparticles. The maximum absorption wavelength of Rhodamine B is 558 nm. During photo catalysis, holes in the valance band react with the adsorbed water molecules and surface bound hydroxyl group(OH^-) and generate hydroxyl radicals (OH*). A super oxide radical anion(O_2^{-*}) was formed by the reduction in oxygen molecules by conduction band electrons. The dye was then degraded by OH* and O_2^{-*} radicals [48]. Degradation reaction steps were as below:

$$NiO + h\vartheta \longrightarrow e^- + h^+$$

$$h^+ + H_2O \longrightarrow H^+ + OH^-$$

$$h^+ + OH^- \longrightarrow OH^*$$

$$e^+ + O_2 \longrightarrow O_2^{*-}$$

$$OH^* + O_2^{*-} + \text{Rh B dye} \longrightarrow \text{Degraded products}$$

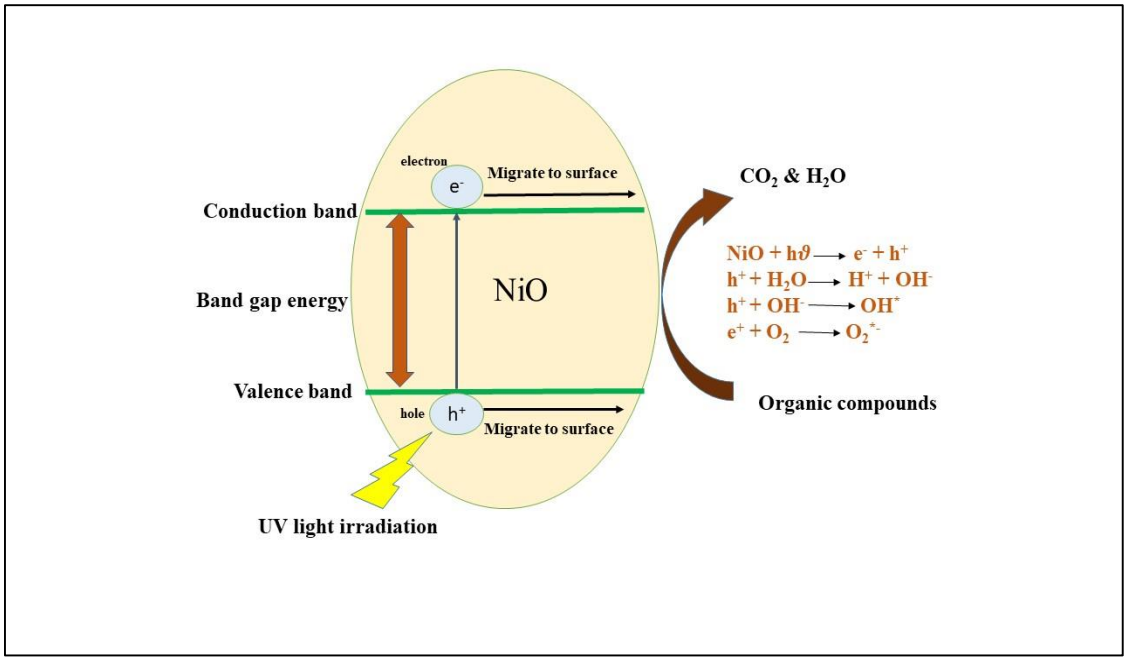

Figure.5.6 Schematics of photocatalytic dye degradation using NiO

From the adsorption-desorption equilibrium analysis, we could infer that our sample achieved equilibrium faster in a lower time limit. The band gap and crystallite size values of NiO were found appropriate for photocatalytic degradation of dye. The photocatalytic degradation curve of Rhodamine B dye by NiO photo catalyst is shown in Figure.5.7

The photocatalytic degradation of Rhodamine B dye using NiO as a photocatalyst can be calculated from equation

$$\textbf{\% of degradation} = \frac{(C_0 - C_e)}{C_0} \times 100$$

Where C_0 is initial concentration of the dye and C_e is final concentration of the dye after the irradiation. The percentage of dye degradation is found to be 89% after 60 minutes. This value showed that the synthesized NiO possess a better photo degradation efficiency for Rhodamine B dye and it showed that particles synthesized at higher temperature also hold good degradation efficiency than those with low temperature [51].

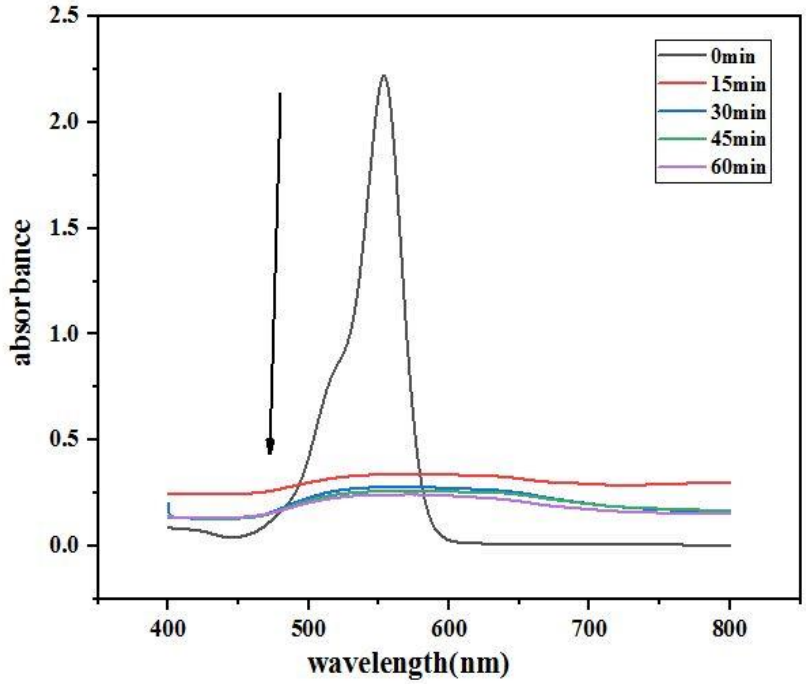

Figure.5.7 Photo catalytic degradation curve of RhB dye using NiO nanoparticle as photocatalyst

The first order kinetic model was applicable in the case of linear fitting of ln (C_e/C_0) with t given by,

$$\ln\left(\frac{C_e}{C_0}\right) = -kt$$

C_0 is the initial concentration and Ce is the concentration after the solar irradiation and t is the time and k is the observed first order rate constant (min^{-1}). The dependence of ln (C_e /C_0) as a function of t was approximated by straight lines. The dye was undergone complete degradation after 60 minutes. The correlation value for the kinetic curves of reaction with R^2 value 0.92143 and rate constant of 0.00709 min^{-1} is given in Figure.5.7.

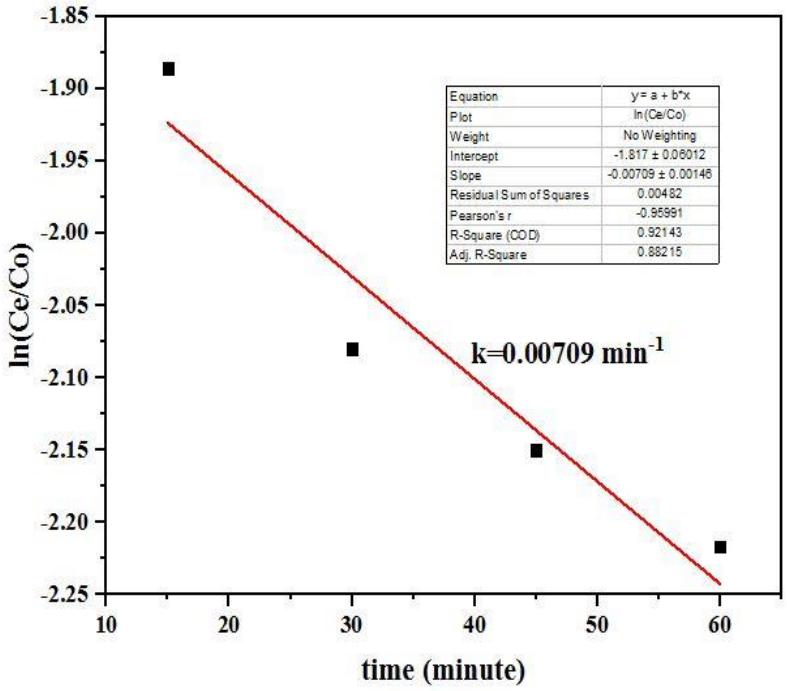

Figure.5.8 ln (C_e /C_0) vs. time rate curve of RhB using NiO as photocatalyst

The percentage of dye degradation increases with time indicating the better performance of NiO (Figure.5.8). The smaller particle size has larger surface-to-volume ratio and shows a greater phonon absorption on the surface of photo catalyst [46].

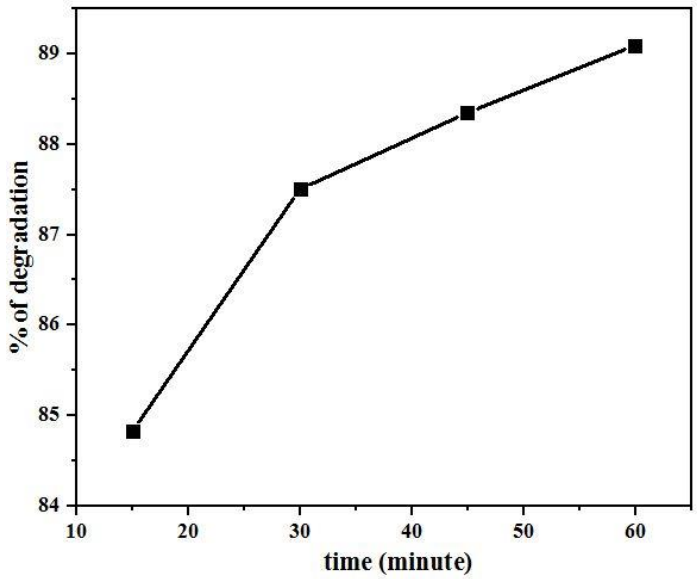

Figure.5.9 Percentage of degradation of RhB dye using NiO as photocatalyst

CHAPTER 6

CONCLUSION AND FUTURE SCOPE

6.1 Conclusion

Here in the present study, I have synthesized the NiO nanoparticles by hydrothermal method using Nickel Nitrate and Sodium Hydroxide as precursors. With the application of temperature of about 180˚C and 24 h, I have obtained $Ni(OH)_2$ as the product. A calcination of about 500˚C for 3 h produced a good crystalline NiO nanoparticles. Structural optical and morphological studies are established that the prepared NiO nanoparticle. XRD spectra with Rietveld refinement revealed that NiO nanoparticle hold a face centered cubic structure with a crystalline size of 17.88 nm. Optical analysis using UV-Visible spectroscopy analysis shows that NiO nanoparticle hold a good optical characteristic with a bandgap of about 3.81 eV confirmed from bandgap analysis. FESEM images shows an oval morphology for the prepared NiO. Then I applied this prepared NiO as a photocatalyst for the degradation of RhB under natural sunlight. The photocatalytic dye degradation studies show that the prepared NiO act as a good photo catalyst with a degradation efficiency of 89 % in 60 min. Higher rate constant and good degradation efficiency in such a lower time limit reveals the efficiency of our synthesized material for the dye degradation application. It is clear that the prepared NiO photocatalyst can be able to use as a good photocatalytic material in a cost-effective manner for the protection of aquatic environment and for controlling environmental problems in the near future.

6.2 Future Scopes

- Application of NiO photocatalyst for other toxic dyes in order to prove it as an efficient environmental friendly photocatalytic material.
- To employ the NiO nanoparticles synthesized at higher temperature and duration in hydrothermal method for other applications including biomedical, energy storage, sensing, etc.
- To analyze the effect of hydrothermal conditions in the structural, optical and morphological properties of NiO.

- To prepare a binary and a ternary hetero structure of NiO with other transition metal oxide and conducting polymers for the application in photocatalysis and other related applications.

.

REFERENCES

[1] K K Chattopadhyay and A N Banerjee, *Introduction to Nanoscience and Nanotechnology*, PHI Learning Private Limited, **1** (2009) 1-5.

[2] A K Lalitha, I.V. Viswanath, S D Bhagavathula, B Govindh, Y L N Murthy *Materials Today: Proceedings* **18** (2019) 2182-2190.

[3] P N Sudha, K Sangeetha, K Vijayalakshmi and A Barhoum, *Emerging Applications of Nanoparticles and Architectural Nanostructure* **12** (2018) 341-384.

[4] M Faraday, *The Bakerian lecture: experimental relation of gold to light*, *Philos. Trans. Roy. Soc*. Lond (1857).

[5] R P Feynman, *There's Plenty of Room at the Bottom: An Invitation to Enter a New Field of Physics*. In: Handbook of Nanoscience, Engineering, and Technology, (2012).

[6] M Nasrollahzadeh, S M Sajadi, M Sajjadi and Z Issaabadi, *Interface Science and Technology* **28** (2019) 1-27.

[7] N Taniguchi, *On the basic concept of "nano-technology", In: Proc. Intl. Conf. Prod. Eng, Part II*, (1974).

[8] K Ibrahim, S Khalid and K Idrees, *Arabian Journal of Chemistry* **12** (2019) 908-931.

[9] A M Ealias and M P Saravanakumar ,*IOP Conf. Series: Materials Science and Engineering* **263** (2017).

[10] T Y Poh, N A ´B Mohamd Ali, M M Aogáin, K M Kathawala, S I Magdeil, W N Kee and H C Sanjay, *Part Fibre Toxicol* **15** (2018).

[11] B Cristina, I P Ivan and R Kevin, *Biointerphases* **2** (2017).

[12] Areola Adedapo Oluwasanu, Fapohunda Oluwaseua, Jimoh Adeleke, Ige Ayikunle and Ogunyele Abhibok Chris, *Scientific applications and prospects of nanomaterials: A Multidisciplinary review*, **18** (2019), 946-961.

[13] Drexler, K. E., *Nanosystems, John Wiley and Sons,* NY, (1992).

[14] Kendal K., *Science, Atlantic publishers* (1994).

[15] Dan Guo, Guoxinxie and Jianbin Luo, *Mechanical properties of nanoparticles basics and applications*, **47** (2013), 013001.

[16] Vardan Galstyan, Manohar P. Bhandari, Veronica Sberveglieri, Giorgio Sberveglieri, and Elisabetta Comini, *Metal oxide Nanostructures in food Applications: Quality control and packing* **6** (2018), 16.

[17] M.M. Byranvand, A.N. Kharat, L. Fatholahi, Z.M. Beiranvand, *A review on synthesis of nano-TiO2 via different methods, J. Nanostruct*. **3** (2013), 1-9

[18] Promod Kumar, W.D.Roos, *Nanoscale Compound Semiconductors and their Optoelectronics Applications*, (2022).

[19] Schubert, Ulrich. and Hüsing, Nicola. (2012) *Synthesis of inorganic materials Weinheim: Wiley-VCH*, page 161.

[20] P. IyyappaRajan, J. Judith Vijaya, S.K. Jesudoss, K. Kaviyarasu, L. John Kennedy,R. Jothiramalingam, Hamad A. Al-Lohedan, Mansoor-Ali Vaali-Mohammed, *Greenfuel-mediated synthesis of self-assembled NiO nano-sticks for dual applications -photocatalytic activity on Rose Bengal dye and antimicrobial action on bacterial strains, Materials Research Express* **4** (**8**) (2017) 085030.

[21] Wang Pei-Pei, Zhang Chen-Xi, Hu Li-Na, Li Shi-Qi, Ren Wei-Hua, Hao Yu-Ying, *Acta Phys. Sin*., **70** (2021).

[22] https://en.wikipedia.org/wiki/Nickel%28II%29_oxide

[23] https://www.azonano.com/article.aspx?ArticleID=3378

[24] Fereshteh Motahari, Mohammad Reza Mozdianfard, Faezeh Soofivand and Masoud Salavati-Niasari, *NiO Nanostructures: Synthesis, Characterization and Photocatalyst Application in Dye Pollution Wastewater Treatment, RSC Advances*.

[25] F. Augusto, E. Carasek, R. G. C. Silva, S. R. Rivellino, A. D. Batista and E. Martendal, *New Sorbents for Extraction and Microextraction Techniques, Journal of Chromatography A*, Vol. **1217**, (2010),2533-2542

[26] SV Ganachari, R Bhat, R Deshpande, A Venkataraman - *Recent Research in Science and Technology*, (2012).

[27] Kien Nguyen, Nguyen Duc Hoa, Chu Manh Hung, Dang Thi Thanh Le,Nguyen Van Duy and Nguyen Van Hieu, *A comparative study on the electrochemical properties of nanoporous nickel oxide nanowires and nanosheets prepared by a hydrothermal method*, *RSC Adv*.,**8** (2018), 19449.

[28] R. Kumar P, N. Prasad, F. Veillon, W. Prellier, *Raman spectroscopic and magnetic properties of Europium doped nickel oxide nanoparticles prepared by microwave assisted hydrothermal method, Journal of Alloys and Compounds* (2020).

[29] Xueliang Li , Xiaoxi Zhang,Zirong Li ,Yitai Qian, *Synthesis and characteristics of NiO nanoparticles by thermal decomposition of nickel dimethylglyoximate rods, Solid State Communications* **137** (2006) 581–584.

[30] Zahra Sabouri, Alireza Akbari, Hasan Ali Hosseini, Majid Darroudi, *Facile green synthesis of NiO nanoparticles and investigation of dye degradation and cytotoxicity effects, Journal of Molecular Structure* (2018).

[31] D. Princess Jeba, T. Peter Amaladhas, *Green synthesis and photocatalytic activity of nickel oxide nanostructures in the degradation of organic dyes, International Journal of Research in Advent Technology*,.**6**, (2018).

[32] Zohra Nazir Kayani, Mahek Zaheen Butt, Zaira Riaz, Shahzad Naseem, *Synthesis of NiO nanoparticles by sol-gel technique, Materials Science*-Poland.

[33] Amgad S. Danial, M.M. Saleh, S.A. Salih, M.I. Awad, *On the synthesis of nickel oxide nanoparticles by sol-gel technique and its electro catalytic oxidation of glucose, Journal of Power Sources*.

[34] Aisha Shamim, Zaheer Ahmad, Sajid Mahmood, Umair Ali, Tariq Mahmood and Zamir Ahmad Nizami, *Synthesis of nickel nanoparticles by sol-gel method and their characterization, Open Journal of Chemistry*.

[35] K. S. Usha, R. Sivakumar, and C. Sanjeeviraja, *Optical constants and dispersion energy parameters of NiO thin films prepared by radio frequency magnetron sputtering technique ,Journal of Applied Physics* **114**, (2013), 123501.

[36] Nurul Nadia Mohd Zorkiplia, Noor Haida Mohd Kausb, Ahmad Azmin Mohamada, *Synthesis of NiO Nanoparticles through Sol-gel Method,Procedia Chemistry* **19** (2016), 626 – 631.

[37] M. Alagiri, S. Ponnusamy, C. Muthamizhchelvan, *Synthesis and characterization of NiO nanoparticles by sol–gel method, J Mater Sci: Mater Electron* **23** (2012),728–732.

[38] G. Jayakumar, A. Albert Irudayaraj, A. Dhayal Raj, *Photocatalytic Degradation of Methylene Blue by Nickel Oxide, Materials Today: Proceedings* **4** (2017) 11690–11695.

[39] D. Mohammadyani, S.A Hosseini, S.K Sadrnezhaad, *Characterisation of Nickel Oxide nanoparticles synthesized via rapid microwave assisted route, International Journal of Modern Physics: Conference Series*. **5** (2012),270–276.

[40] Lay Gaik Teoh and Kun-Dar Li, *Synthesis and Characterization of NiO Nanoparticles by Sol-Gel Method, Materials Transactions*, **53** (2012), 2135 to 2140.

[41] B D Cullity, *Elements of X-ray Diffraction, Second Edition*, Addison-Wesley Publishing company **3** (1978), 81-82.

[42] M A Omar, *Elementary Solid State Physics: Principles and Applications*, Addison-Wesley Publishing Company **2** (1975), 34-60.

[43] Brian D.Viezbicke, ShanePatel, *Evaluation of the Tauc method for optical absorption edge determination: ZnO thin film as a model system*, **252** (2015), 1700-1710.

[44] https://serc.carleton.edu/research_education/geochemsheets/techniques/SEM.html

[45]https://www.purdue.edu/ehps/rem/laboratory/equipment%20safety/Research%20Equipment/sem.html

[46] Susmi Anna Thomas, Sujit Anil Kadam,Yuan-Ron Ma, and Arun Aravind, *Photocatalytic Degradation of Malachite Green Dye Using Zinc Sulfide Nanostructures, Materials Science inc. Nanomaterials & Polymers.*

[47] M. El-Kemary, N. Nagy, I. El-Mehasseb, *Nickel oxide nanoparticles: Synthesis and spectral studies of interactions with glucose, Materials Science in Semiconductor Processing*.

[48] Sujit Anil Kadam , Susmi Anna Thomas, Yuan-Ron Ma, Lolly Maria Jose , D. Sajan , Arun Aravind, *Investigation of adsorption and photocatalytic behavior of manganese 4 doped zinc oxide nanostructures, Inorganic Chemistry Communications*.

[49] Pothapalayam Mahali Ponnusamy, Santhanam Agilan,Natarajan Muthukumarasamy, and Dhayalan Velauthapillai, *Effect of Chromium and Cobalt Addition on Structural, Optical and Magnetic Propertiesof NiO Nanoparticle,Z. Phys. Chem*. 2015.

[50]https://www.researchgate.net/post/Why_the_properties_will_be_changed_in_NiO_when_we_goes_from_from_bulk_transition_metal_oxide_to_nano_range_semiconductor#:~:text=NiO%20is%20a%20p-type%20semiconductor%20with%20a%20band,due%20to%20the%20confinement%20of%20electrons%20and%20holes.

[51] Mohamed Abboud, Mohammad Abu Haija, Radhaoune Bel-Hadj-Tahar, Ahmed t. Mubarak, Issam Ismail, Mohamed S. Hamdy, *Highly ordered mesoporous flower- like NiO nanoparticles: Synthesis, characterization and photocatalytic performance, New Journel of Chemistry.*